THE FASEB JOURNAL • RESEARCH • www.fasebj.org

Cilantro leaf harbors a potent potassium channel–activating anticonvulsant

Rían W. Manville and Geoffrey W. Abbott[1]

Bioelectricity Laboratory, Department of Physiology and Biophysics, School of Medicine, University of California–Irvine, Irvine, California, USA

ABSTRACT: Herbs have a long history of use as folk medicine anticonvulsants, yet the underlying mechanisms often remain unknown. Neuronal voltage-gated potassium channel subfamily Q (KCNQ) dysfunction can cause severe epileptic encephalopathies that are resistant to modern anticonvulsants. Here we report that cilantro (*Coriandrum sativum*), a widely used culinary herb that also exhibits antiepileptic and other therapeutic activities, is a highly potent KCNQ channel activator. Screening of cilantro leaf metabolites revealed that one, the long-chain fatty aldehyde (E)-2-dodecenal, activates multiple KCNQs, including the predominant neuronal isoform, KCNQ2/KCNQ3 [half maximal effective concentration (EC_{50}), 60 ± 20 nM], and the predominant cardiac isoform, KCNQ1 in complexes with the type I transmembrane ancillary subunit (KCNE1) (EC_{50}, 260 ± 100 nM). (E)-2-dodecenal also recapitulated the anticonvulsant action of cilantro, delaying pentylene tetrazole-induced seizures. *In silico* docking and mutagenesis studies identified the (E)-2-dodecenal binding site, juxtaposed between residues on the KCNQ S5 transmembrane segment and S4-5 linker. The results provide a molecular basis for the therapeutic actions of cilantro and indicate that this ubiquitous culinary herb is surprisingly influential upon clinically important KCNQ channels.—Manville, R. W., Abbott, G. W. Cilantro leaf harbors a potent potassium channel–activating anticonvulsant. FASEB J. 33, 11349–11363 (2019). www.fasebj.org

KEY WORDS: herbal medicine · epilepsy · KCNQ1 · KCNQ2 · KCNQ3

Documented use of botanical folk medicines stretches back as far as recorded human history itself (1). There is DNA evidence suggestive of consumption of plants for medicinal use by *Homo neanderthalensis* 48,000 yr ago (2, 3), and there is archaeological evidence of nonfood use by *Homo erectus* or similar species up to 800,000 yr ago of herbs used in the modern era as folk medicines (4). Evidence for the efficacy of such medicines ranges from anecdotal to clinical trials; similarly, mechanisms and active compounds have been elucidated for some botanical medicines, whereas for others the molecular basis of action is unknown (5, 6).

In many cases, botanical medicines of current or historical use are also currently consumed, often on a large scale, as foodstuffs or food flavoring. One example is cilantro (*Coriandrum sativum*), known as coriander in the United Kingdom (**Fig. 1*A***). Cilantro has been consumed by human beings for at least 8000 yr (based on archaeological evidence from what is now Israel) and was found in the tomb of Tutankhamen and is thought to have been cultivated by the ancient Egyptians (7). Cilantro now grows wild over broad expanses of the globe, and its leaves feature heavily in Asian, European, and Central American cuisine. Cilantro also has reported anticancer, anti-inflammatory, antifungal, antibacterial, anticonvulsant, cardioprotective, gastric health, and analgesic effects (8). In many cases, the molecular basis and active components of the various therapeutic effects of cilantro are incompletely understood or unknown.

Voltage-gated potassium (Kv) channels within the Kv channel subfamily Q (KCNQ), also termed the Kv7 subfamily, are sensitive to activation by a range of small molecules, including synthetic drugs, neurotransmitters, and metabolites (9–13). Kv channels, including the 5 isoforms within the KCNQ (Kv7) subfamily, are composed of tetramers of pore-forming (α) subunits, each consisting of 6 transmembrane segments (S): S1–4 comprise the voltage-sensing domain (VSD), and S5–6 comprise the pore module (Fig. 1*B*). Kv channels respond to cell membrane depolarization *via* movement of their VSD, which causes pore opening and K^+ diffusion (predominantly outward) through the pore, reducing

ABBREVIATIONS: EC_{50}, half maximal effective concentration; KCNA1, voltage-gated potassium channel subfamily A member 1; KCNE1, voltage-gated potassium channel subfamily E; KCNQ, voltage-gated potassium channel subfamily Q; Kv, voltage-gated potassium; PTZ, pentylene tetrazole; TEVC, 2-electrode voltage-clamp; VSD, voltage-sensing domain

[1] Correspondence: Department of Physiology and Biophysics, Bioelectricity Laboratory, Medical Sciences D337, ZOT 4560, School of Medicine, University of California–Irvine, Irvine, CA 92697, USA. E-mail: abbottg@uci.edu

doi: 10.1096/fj.201900485R

This article includes supplemental data. Please visit *http://www.fasebj.org* to obtain this information.

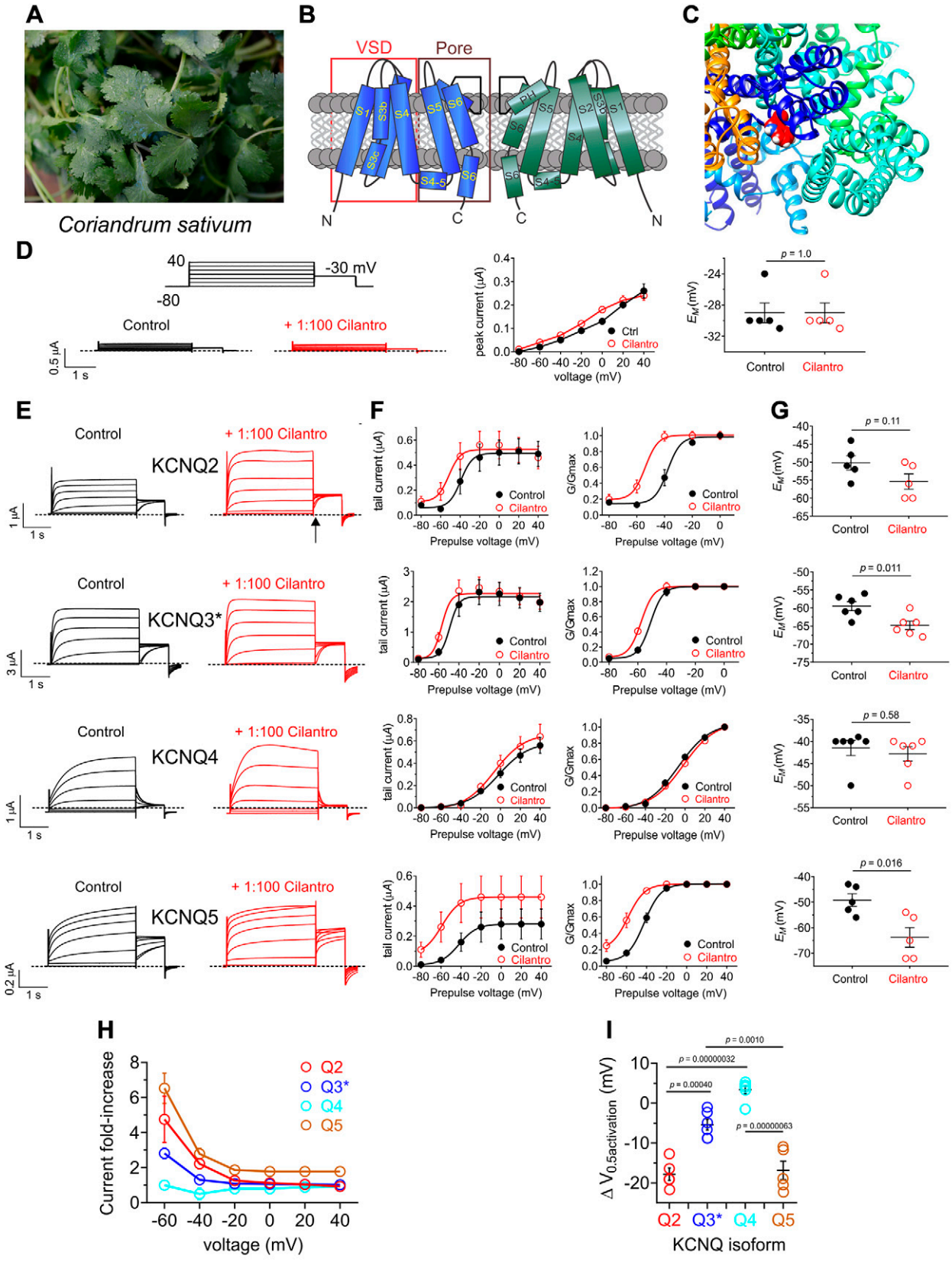

Figure 1. Cilantro extract differentially activates homomeric KCNQ channels All error bars indicate SEM. *A*) Image of the fresh cilantro (*Coriander sativum*) used in this study. *B*) Topological representation of a Kv channel showing 2 of the 4 subunits that comprise a channel. *C*) Extracellular view of the chimeric KCNQ1/KCNQ3 structural model to highlight the anticonvulsant binding pocket (red, KCNQ3-W265). *D*) Left, mean TEVC current traces for water-injected *Xenopus* oocytes in the absence (control) or presence of 1% cilantro extract ($n = 5$). Dashed line here and throughout indicates the 0 current level. Upper inset:

(*continued on next page*)

action potential frequency or repolarizing the cell following action potential firing. Kv channels can also be activated, or their voltage dependence of activation shifted toward more negative potentials, by a number of small molecules, including specific drugs. In the case of neuronally expressed KCNQ channels, molecules such as the anticonvulsant retigabine bind to a pocket between the VSD and pore (Fig. 1C) to activate the channel by favoring opening at more hyperpolarized potentials; this has antiepileptic effects by raising the barrier for neuronal firing (14).

The KCNQ family exhibits a wide range of tissue expression and functional attributes; KCNQ channels are therefore highly influential in many aspects of human physiology. Heteromeric KCNQ2/3 and also KCNQ3/5 channels generate the muscarinic receptor–inhibited M-current, a subthreshold Kv current that regulates neuronal firing; homomeric KCNQ2, KCNQ3, and KCNQ5 channels may also contribute (15–19). Activation of KCNQ1, KCNQ4, and KCNQ5 channels expressed in vascular smooth muscle reduces vascular tone (20). KCNQ1 is also expressed in the human heart, the inner ear, and a variety of epithelia (21); KCNQ4 is expressed in auditory neurons and hair cells (22) and, like KCNQ1 (23), is essential for hearing.

Given the sensitivity of KCNQ channels to various small molecules and their diverse expression and functional roles, many of which potentially match the purported therapeutic effects of cilantro, here we screened KCNQ channels for sensitivity to cilantro. We discovered that cilantro activates various KCNQ isoforms and identified a single cilantro metabolite (and its KCNQ channel binding site) that underlies the KCNQ-activating and anticonvulsant properties of cilantro.

MATERIALS AND METHODS

Preparation of plant extracts

Certified organic fresh cilantro (*Coriandrum sativum*) was sourced from Mother's Market and Kitchen (Irvine, CA, USA), and homogenized fresh using a blender (SharkNinja, Needham, MA, USA). We then performed a methanolic extraction (80% methanol/20% water) on the cilantro homogenate for 48 h at room temperature on a rocking platform with occasional inversion of the bottles to more fully resuspend the extract. Following this process, the extract was filtered using Whatman filter paper #1 (Whatman, Maidstone, United Kingdom), and then the methanol was removed by evaporation in a fume hood for 48 h at room temperature. The extract was then centrifuged for 10 min at 15°C, 4000 relative centrifugal force to remove remaining particulate matter, followed by storage at −20°C. On the day of electrophysiological recording, the cilantro extract was thawed and then diluted 1:100 in bath solution immediately before use.

Channel subunit cRNA preparation and *Xenopus laevis* oocyte injection

As previously described (12), we generated cRNA transcripts encoding human Kv channel subfamily A member 1 (KCNA1), Kv channel subfamily E member 1 (KCNE1), KCNE2, KCNE3, KCNQ1, KCNQ2, KCNQ3, KCNQ4, or KCNQ5 by *in vitro* transcription using the T7 polymerase mMessage mMachine Kit (Thermo Fisher Scientific, Waltham, MA, USA), after vector linearization, from cDNA subcloned into plasmids incorporating *Xenopus laevis* β-globin 5′ and 3′ UTRs flanking the coding region to enhance translation and cRNA stability. We quantified cRNA by spectrophotometry. We generated mutant KCNQ2 and KCNQ3 cDNAs by site-directed mutagenesis with a QuikChange Kit (StrataGene California, San Diego, CA, USA) and prepared the cRNAs as above. We injected defolliculated stage V and VI *X. laevis* oocytes (Ecocyte Bioscience, Austin, TX, USA, and Xenoocyte, Dexter, MI, USA) with KCNE or KCNQ cRNAs (5–20 ng), or both. We incubated the oocytes at 16°C in Barth's saline solution (Ecocyte Bioscience) containing penicillin and streptomycin, with daily washing, for 3–5 d prior to 2-electrode voltage-clamp (TEVC) recording.

TEVC

We performed TEVC at room temperature using an OC-725C amplifier (Warner Instruments, Hamden, CT, USA) and pClamp10 software (Molecular Devices, San Jose, CA, USA) 2–5 d after cRNA injection as described in the section above. For recording, we placed the oocytes in a small-volume oocyte bath (Warner Instruments) and viewed them with a dissection microscope. We sourced chemicals from MilliporeSigma (Burlington, MA, USA) unless otherwise stated. We studied the effects of 1% cilantro extract and of 9 compounds previously identified in cilantro extract. Vanillic acid and 3,4-dihydroxybenzoic acid were each solubilized in 100% ethanol at a stock concentration of 100 mM; the other compounds were solubilized directly in bath solution. We initially screened for KCNQ2/3 channel activity using 100 μM concentrations of each of the 9 components, then conducted dose responses where appropriate. Bath solution was (mM): 96 NaCl, 4 KCl, 1 $MgCl_2$, 1 $CaCl_2$, 10 4-(2-hydroxyethyl)-1-piperazineethanesulfonic acid (pH 7.6). We introduced 1% cilantro extract, or each of the 9 cilantro components, into the oocyte recording bath by gravity perfusion at a constant flow of 1 ml/min for 3 min prior to recording. Pipettes were of 1–2 MΩ

the voltage protocol used here and throughout the study unless otherwise indicated. Center: mean tail current for oocytes on left ($n = 5$). Right: scatter plot of resting membrane potential (E_M) of water-injected oocytes in the absence (Control) or presence of cilantro extract ($n = 5$). Statistical analyses by 2-way ANOVA. *E*) Left: mean TEVC current traces for *Xenopus* oocytes expressing the KCNQ homomers indicated in the absence (control) or presence of 1% cilantro extract ($n = 5$–6). Arrow indicates time point at which KCNQ tail currents are measured throughout this study. *F*) Mean tail current (left) and normalized tail current (G/G_{max}) (right) *vs.* prepulse voltage relationships for the traces as in the previous panel ($n = 5$–6). *G*) Effects of 1% cilantro extract on E_M of unclamped oocytes expressing the channels as in *E* ($n = 5$–6). Statistical analyses by 2-way ANOVA. *H*) Current-fold increase *vs.* voltage for the KCNQ isoforms indicated, induced by 1% cilantro extract ($n = 5$–6). *I*) Scatter plot showing mean $\Delta V_{0.5\ activation}$ induced by 1% cilantro extract for the KCNQ isoforms indicated ($n = 5$–6). Statistical analysis by 2-way ANOVA corrected for multiple comparisons.

resistance when filled with 3 M KCl. We recorded currents in response to voltage pulses between −120 or −80 mV and +40 mV at 20-mV intervals from a holding potential of −80 mV, to yield current-voltage relationships, current magnitude, and for quantifying activation rate. We analyzed data using Clampfit (Molecular Devices) and Prism software (GraphPad, La Jolla, CA, USA); values are stated as means ± SEM. We plotted raw or normalized tail currents *vs.* prepulse voltage and fitted with a single Boltzmann function:

$$g = \frac{(A_1 - A_2)}{\left\{1 + \exp[V_{\frac{1}{2}} - V \Big/ V_s]\right\} y + A_2} \quad (1)$$

where g is the normalized tail conductance, A_1 is the initial value at $-\infty$, A_2 is the final value at $+\infty$, $V_{1/2}$ is the half-maximal voltage of activation, and V_s is the slope factor. We fitted activation and deactivation kinetics with single exponential functions.

Chemical structures and *silico* docking

We plotted and viewed chemical structures and electrostatic surface potential using Jmol, an open-source Java viewer for chemical structures in 3 dimensions (*http://jmol.org/).* For *in silico* ligand docking predictions of binding to KCNQ2, we first altered the *Xenopus laevis* KCNQ1 cryo-electron microscopy–derived structure (PDB 5VMS) (24) to incorporate KCNQ2 residues important for retigabine binding, and their immediate neighbors, followed by energy minimization as we previously described (12) using the GROMOS (*http://www.gromacs.org/Documentation/Terminology/Force_Fields/GROMOS*) 43B1 force field (25) in DeepView (*https://spdbv.vital-it.ch/*) (26). We then performed unguided docking of (E)-2-dodecanal to predict potential binding sites, using SwissDock (*http://www.swissdock.ch/*) with CHARMM (*https://www.charmm.org/charmm/?CFID=ed8a7ee0-fc9b-441f-80aa-a802ce55866e&CFTOKEN=0*) force fields (27, 28). We used a similar approach to simulate binding to KCNQ1 and KCNQ1/KCNE1 but instead employed closed- and open-state models of either channel previously developed by Kang *et al*. (29).

Pentylene tetrazole chemoconvulsant assay

We quantified the anticonvulsant activities of (E)-2-dodecenal and tridecanal in male C57BL/6 mice (Charles River Laboratories, Wilmington, MA, USA) aged 2–3 mo. The mice were housed and used according to the recommendations in the *Guide for the Care and Use of Laboratory Animal*s (National Institutes of Health, Bethesda, MD, USA). The study protocol was approved by the Institutional Animal Care and Use Committee of University of California−Irvine. The chemicals were sourced from MilliporeSigma. We used a pentylene tetrazole (PTZ) chemoconvulsant assay as previously described (30). We injected the mice intraperitoneally with (E)-2-dodecenal (2 or 20 mg/kg) (with or without 2.5 mg/kg XE991) or tridecanal (20 mg/kg) solubilized in PBS, or vehicle control (PBS), and then 30 min later we injected mice intraperitoneally with 80 mg/kg PTZ. Following the PTZ injection, the mice were caged individually, and an observer (GWA) blinded to the experimental condition timed the latency to first seizure.

Statistical analysis

All values are expressed as means ± SEM. One-way ANOVA was applied for all tests; all P values were 2-sided. Where appropriate, we applied Tukey's correction for multiple comparisons.

RESULTS

Cilantro extract activates multiple KCNQ isoforms

We performed a methanolic extraction (80% methanol/20% water) on fresh cilantro (*Coriandrum sativum*) (Fig. 1*A*). Following removal of the methanol to leave an aqueous solution of cilantro extract, we diluted the extract 1/100 in recording solution and screened for effects first on homomeric neuronal KCNQ channels heterologously expressed in *Xenopus laevis* oocytes using TEVC electrophysiology.

Cilantro extract had no effect on water-injected control oocytes (Fig. 1*D*). In contrast, the cilantro extract exhibited effects on all 4 neuronal KCNQs. In the case of KCNQ2, KCNQ3, and KCNQ5, cilantro negative-shifted the voltage dependence of activation, the strongest effects being on KCNQ2 and KCNQ5 (Fig. 1*E, F*). This produced hyperpolarization in the rest of the cells expressing KCNQ2, KCNQ3* [KCNQ3-A315T, a mutant that passes larger currents than wild-type KCNQ3, facilitating study of the homomeric channel (31)], or KCNQ5 (Fig. 1*G*). Cilantro extract exhibited potentiation of the early phase of KCNQ4 prepulse currents, but this was not reflected in the tail currents and did not result in shifted resting membrane potential (E_M) of KCNQ4-expressing oocytes (Fig. 1*E–G*). Thus, the most cilantro-sensitive neuronal homomers were KCNQ2 and KCNQ5, which were compared by examining both the fold increase in tail current (Fig. 1*H*) and the negative shift in the voltage dependence of activation ($\Delta V_{0.5\ activation}$) (Fig. 1*I* and Supplemental Tables S1–S4); KCNQ5 also exhibited cilantro-dependent increases in peak tail current (Fig. 1*F*, left).

KCNQ2/3 heteromers are the primary KCNQ channel generating M-current in mammalian brain, and the main target of retigabine-class anticonvulsants (9, 13). Here, cilantro extract (1/100) was effective at negative-shifting KCNQ2/3 voltage dependence of activation (**Fig. 2*A*, *B***) and hyperpolarizing KCNQ2/3-expressing cells (Fig. 2*C*).

The other KCNQ family member, KCNQ1, is retigabine-insensitive and is expressed in the human heart and a variety of secretory epithelia, including the gastric glands, colon, and thyroid (21). KCNQ1 is notable for its functional diversity, largely endowed by formation of complexes with KCNE single-transmembrane spanning ancillary subunits. Although homomeric KCNQ1 is functional, it is thought that *in vivo* KCNQ1 always complexes with KCNE subunits (21). In the human heart and inner ear, KCNQ1-KCNE1 complexes form the relatively positive and slowly activating I_{KS} current in ventricular myocytes (32, 33). In contrast, constitutively active KCNQ1-KCNE3 channels are expressed in the colonic epithelium basolateral membrane, where they regulate chloride ion secretion (34). KCNQ1 was also activated by cilantro extract (Fig. 2*D, E*), although this did not influence E_M (Fig. 2*F*) because the KCNQ1 current potentiation occurred across a narrow voltage range, positive to the resting E_M of KCNQ1-expressing oocytes (Fig. 2*E*, left). KCNQ1-KCNE1 was more sensitive, with cilantro inducing a larger increase in current (Fig. 2*D, E*) and hyperpolarizing

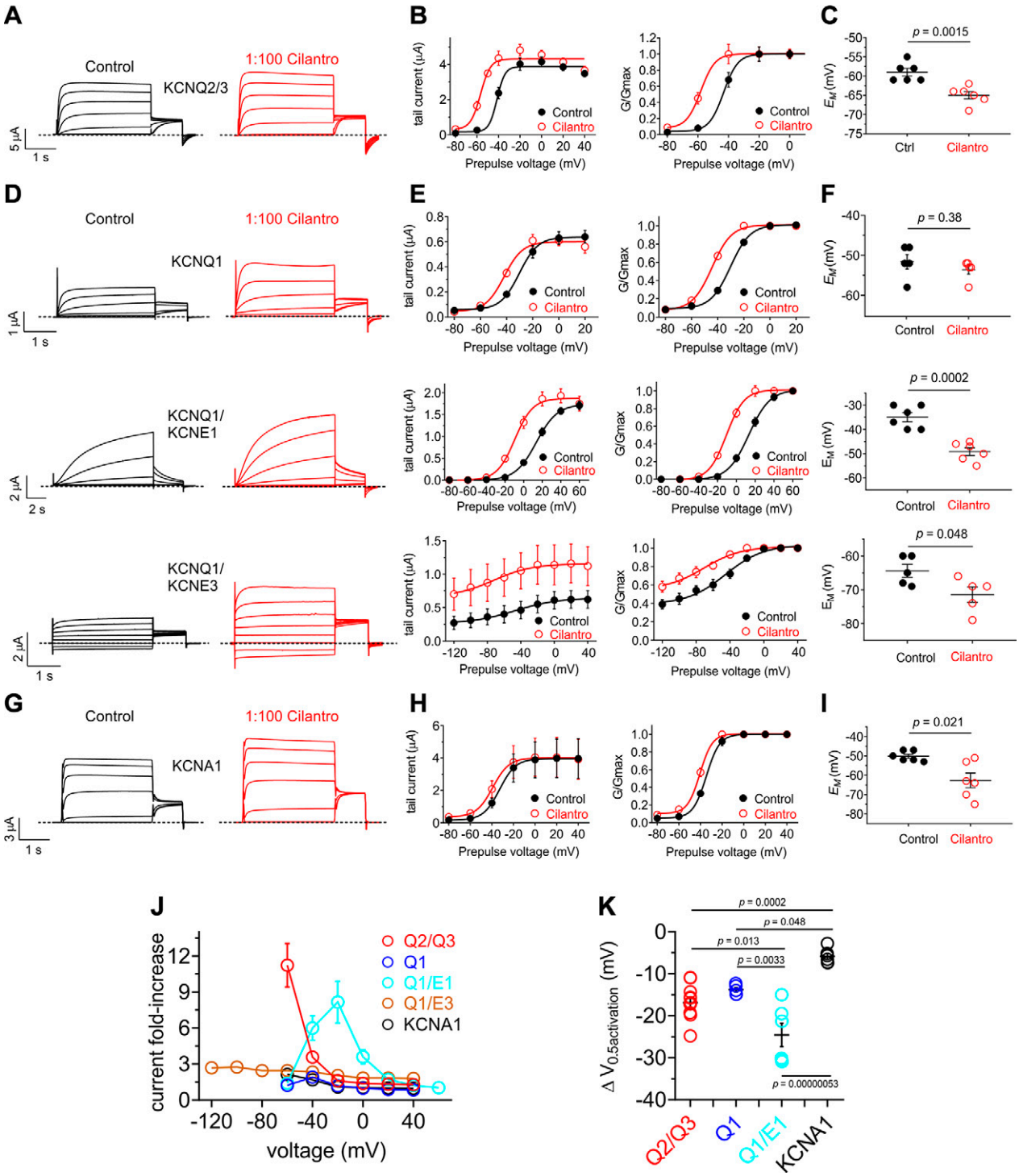

Figure 2. Cilantro extract differentially activates heteromeric KCNQ channels All error bars indicate SEM. *A*) Left, mean TEVC current traces for *Xenopus* oocytes expressing KCNQ2/3 in the absence (control) or presence of 1% cilantro extract ($n = 6$). *B*) Mean tail current (left) and normalized tail current (G/G_{max}) (right) *vs.* prepulse voltage relationships for the KCNQ2/3 traces as in *A* ($n = 6$). *C*) Effects of 1% cilantro extract on E_M of unclamped oocytes expressing KCNQ2/3 ($n = 6$). Statistical analysis by 2-way ANOVA. *D*) Left: mean TEVC current traces for *Xenopus* oocytes expressing homomeric KCNQ1 or heteromeric KCNQ1-KCNE channels as indicated in the absence (control) or presence of 1% cilantro extract ($n = 5$–6). *E*) Mean tail current (left) and normalized tail current (G/G_{max}) (right) *vs.* prepulse voltage relationships for the traces as in *D* ($n = 5$–6). *F*) Effects of 1% cilantro extract on E_M of unclamped oocytes expressing the channels indicated in *D* ($n = 5$–6). Statistical analysis by 2-way ANOVA. *G*) Left: mean TEVC current traces for *Xenopus* oocytes expressing homomeric KCNA1 in the absence (control) or presence of 1% cilantro extract ($n = 6$). *H*) Mean tail current (left) and normalized tail current (G/G_{max}) (right) *vs.* prepulse voltage relationships for the traces as in *G* ($n = 6$). *I*) Effects of 1% cilantro extract on E_M of unclamped oocytes expressing KCNA1 ($n = 6$). Statistical analysis by 2-way ANOVA. *J*) Current-fold increase *vs.* voltage for the Kv channel isoforms indicated, induced by 1% cilantro extract ($n = 5$–6). *K*) Scatter plot showing mean $\Delta V_{0.5\ activation}$ induced by 1% cilantro extract for the Kv channel isoforms indicated; $n = 5$–6. Statistical analysis by 2-way ANOVA corrected for multiple comparisons.

E_M (Fig. 2*F*). Cilantro extract even potentiated activity of the constitutively open KCNQ1-KCNE3 channel, almost 3-fold at −120 mV (Fig. 2*D, E*), also negative-shifting E_M (Fig. 2*F*).

Outside the KCNQ family, cilantro induced a relatively small (−5.9 ± 0.9 mV) shift in the voltage dependence of activation of another neuronally expressed Kv channel, KCNA1 (Kv1.1) (Fig. 2*G, H*) which generated a −10 mV shift in E_M of KCNA1-expressing oocytes (Fig. 2*I*). Comparing 2 parameters of negative-shifted voltage-dependent activation (fold increase in current at −60 mV and $\Delta V_{0.5\ activation}$) for all channels tested, cilantro extract was most effective at potentiating KCNQ2/3 and KCNQ1/KCNE1 activity; effects on KCNQ1/KCNE3 were also notable as they spanned the entire voltage range tested (Fig. 2*J, K* and Supplemental Tables S5–S9).

A single cilantro metabolite recapitulates cilantro activation of KCNQs

We next screened the predominant metabolites found in cilantro extract for KCNQ2/3 opening activity. Strikingly, out of 9 metabolites tested at 100 μM, only 1 activated KCNQ2/3—the 12-carbon fatty aldehyde, (E)-2-dodecenal. This specificity was remarkable given that closely related 10, 11, and [^{13}C] aldehydes did nothing to KCNQ2/3 activity (**Fig. 3*A*–*C***). (E)-2-dodecenal both hyperpolarized the activation of KCNQ2/3 and increased its peak tail current at saturating membrane potentials (Fig. 3*C* and Supplemental Tables S10–S18).

Examining effects on homomeric KCNQs, we found that (E)-2-dodecenal (100 μM) shares a similar efficacy profile to cilantro extract [*i.e.*, it preferentially negative-shifted the $\Delta V_{0.5\ activation}$ of KCNQ2 and KCNQ5 *vs.* KCNQ1, KCNQ3, and KCNQ4 (**Fig. 4*A, B***; summarized in Fig. 4*C*)]. (E)-2-dodecenal most potently activated KCNQ2 [half maximal effective concentration (EC_{50}), 60 ± 10 nM] *vs.* the other isoforms, as shown in the dose response that again highlighted increased efficacy for KCNQ2 and KCNQ5 *vs.* other isoforms (Fig. 4*D* and Supplemental Tables S19–S24). Strikingly, effects of whole cilantro extract on heteromeric KCNQ2/3 channel activation (increased) and deactivation (decreased) rates (Fig. 4*E*) were very similar to those induced by (E)-2-dodecenal (Fig. 4*F* and Supplemental Tables S25–S28), further supporting the conclusion that (E)-2-dodecenal is the molecular basis for cilantro activation of KCNQ channels. Importantly, a previous study of the composition of cilantro sourced from the United States identified (E)-2-dodecenal as the primary component, at 15.6%, of essential oil derived from the leaves (35).

Cilantro confers a variety of beneficial effects (8), several of which could potentially involve KCNQ activation. Here, we focused on its effects as an anticonvulsant. Prior work showed that cilantro extract delays the onset (increases latency) of PTZ-induced seizures in rats without altering the overall incidence of clonic or tonic seizures (36). We compared the effects on PTZ-induced seizure latency in mice of (E)-2-dodecenal (2 and 20 mg/kg) *vs.* the closely structurally related, KCNQ2/3-inactive, tridecanal (20 mg/kg). We found that, strikingly, (E)-2-dodecenal increased the latency to first seizure >3-fold ($P = 0.0021$; $n = 15$–29) at 20 mg/kg and almost 3-fold at 2 mg/kg ($P = 0.06$; $n = 16$–20), whereas tridecanal (20 mg/kg) had no effect ($P = 0.40$; $n = 15$), *vs.* day- and age-matched controls for each cohort injected with PBS (Fig. 4*G*). The 3-fold increase in latency with (E)-2-dodecenal was quantitatively very similar to the increase in latency previously observed by others (36) for whole cilantro hydroalcoholic extract. In additional seizure studies in a separate cohort of mice, we found that the KCNQ family–specific inhibitor, XE991 (2.5 mg/kg), eliminated the protective effect of (E)-2-dodecenal (20 mg/kg) ($P = 0.54$; $n = 13$–14) (Fig. 4*H*).

Together with the effects we observed *in vitro* on KCNQ2/3 and other neuronal KCNQ isoforms, these data support the conclusion that (E)-2-dodecenal is a preeminent component of the anticonvulsant action of cilantro. Additionally, KCNQ3/KCNQ5 channels may also contribute to neuronal M-current, and their dysfunction could participate in epilepsy and other hyperexcitability disorders (37, 38). Here, we found that KCNQ3/KCNQ5 channels are almost as (E)-2-dodecenal–sensitive as KCNQ5 (similar potency, ~30% lower efficacy), in contrast with the insensitive homomeric KCNQ3* (Supplemental Fig. S1*A–D* and Supplemental Tables S24 and S29). Thus, activation of neuronal KCNQ3/KCNQ5 channels could also contribute to the anticonvulsant effects of (E)-2-dodecenal.

(E)-2-dodecenal activates KCNQ2/3 *via* a binding site spanning S5 and the S4-5 linker

(E)-2-dodecenal possesses negative electrostatic surface potential centered at its sole carbonyl oxygen (**Fig. 5*A***). This chemical property was previously found to be a prerequisite for activation and binding by retigabine and its derivatives, and γ-aminobutyric acid, of neuronal KCNQ channels (12, 39), *via* a specific S5 tryptophan (W236 in KCNQ2; W265 in KCNQ3) (40) (Fig. 5*B, C*). KCNQ1 lacks the equivalent tryptophan and is retigabine-insensitive (39). However, KCNQ1 is sensitive to (E)-2-dodecenal (Fig. 4). We previously discovered that a conserved arginine at the foot of the voltage sensor (Fig. 5*C*) mediates KCNQ1 (R243) and KCNQ2/3 (R213/R242) activation by mallotoxin (41). To determine the residues required for (E)-2-dodecenal activation of KCNQs, we first used SwissDock to predict possible binding sites of (E)-2-dodecenal to a chimeric structural model based on the cryo-electron microscopy–derived structure of KCNQ1 (24) but while incorporating residues important for retigabine binding as we previously described (12). SwissDock predicted that (E)-2-dodecenal binds between (KCNQ2 numbering) W236 and R213, closer to and hydrogen bonding with the latter (Fig. 5*D*).

To assess the validity of this prediction, we tested the (E)-2-dodecenal sensitivity of KCNQ2/3 channels with mutation to leucine of KCNQ2-W236 and KCNQ3-W265 (Fig. 5*E, F*) or mutation to alanine of KCNQ2-R213 and KCNQ3-R242 (Fig. 5*G, H*). Effects of (E)-2-dodecenal (100 μM) were robustly diminished by either pair of mutations, quantified either by current-fold increase *vs.* voltage

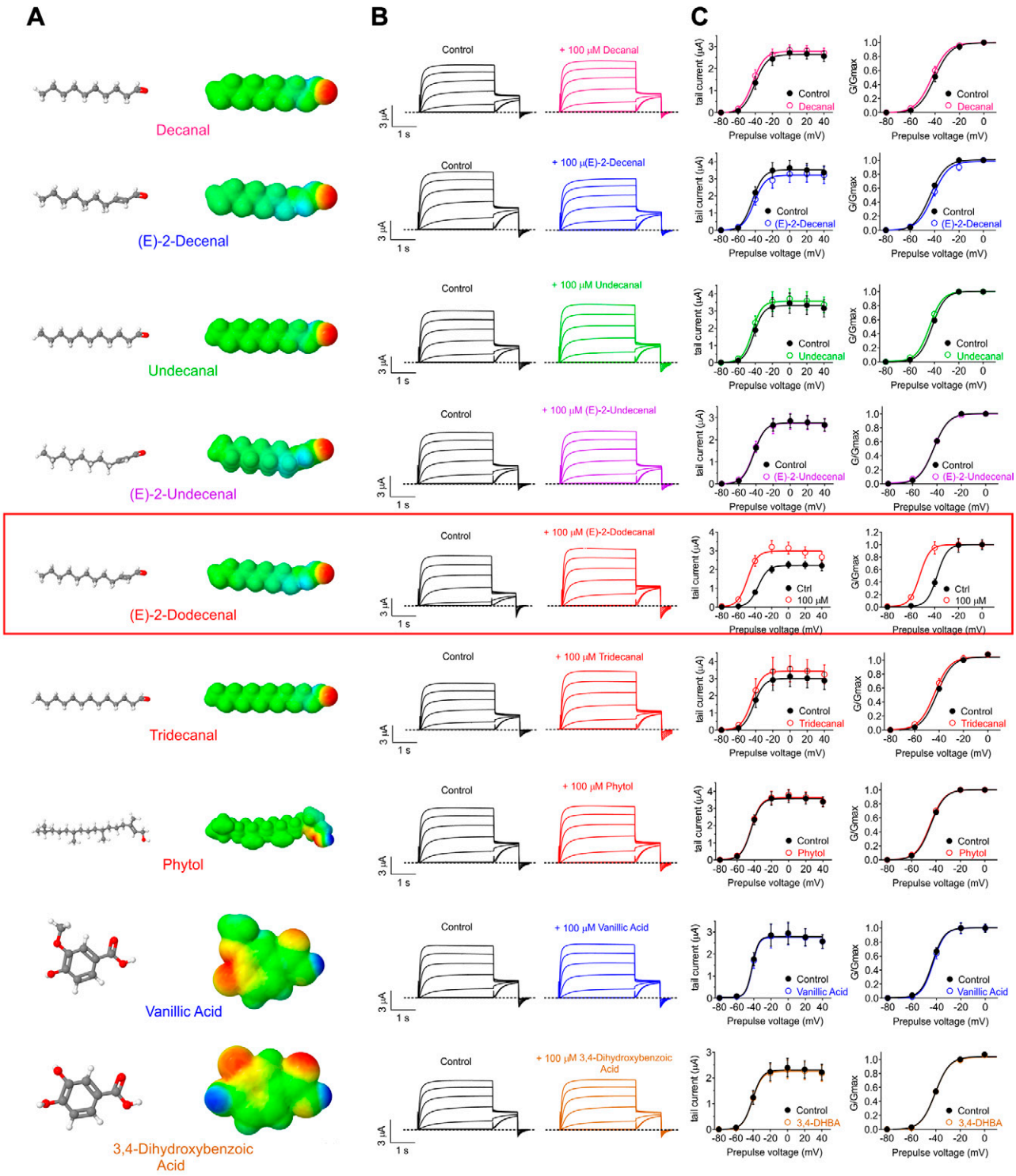

Figure 3. (E)-2-dodecenal is the KCNQ2/3-activating metabolite in cilantro All error bars indicate SEM. Red box indicates the sole hit, (E)-2-dodecenal. *A*) Chemical structures (left; red indicates oxygen) and electrostatic surface plots (right; red, negative; blue, positive) of the cilantro compounds screened in this study. *B*) Mean TEVC current traces showing effects of compounds in *A* (all 100 μM) on KCNQ2/3 expressed in *Xenopus* oocytes (n = 5–11). *C*) Mean tail current (left) and normalized tail currents (G/G_{max}) (right) *vs.* prepulse voltage relationships for the traces as in *B* (n = 5–11). 3,4-DHBA, 3,4-dihydroxybenzoic acid.

(Fig. 5*I*) or $\Delta V_{0.5\ activation}$ (Fig. 5*J*). Similar to wild-type KCNQ2 channels, KCNQ2/3 was highly sensitive to (E)-2-dodecenal, exhibiting an EC_{50} of 60 ± 20 nM. Dose responses for current-fold increase and for $\Delta V_{0.5\ activation}$ showed that either pair of mutations reduced both the potency (14–19-fold) and efficacy of (E)-2-dodecenal effects on KCNQ2/3 channel activation (Fig. 5*K* and Supplemental Tables S24 and S30–S32).

Studying the effects of the W and R mutants on homomeric KCNQ2 channels is problematic because of

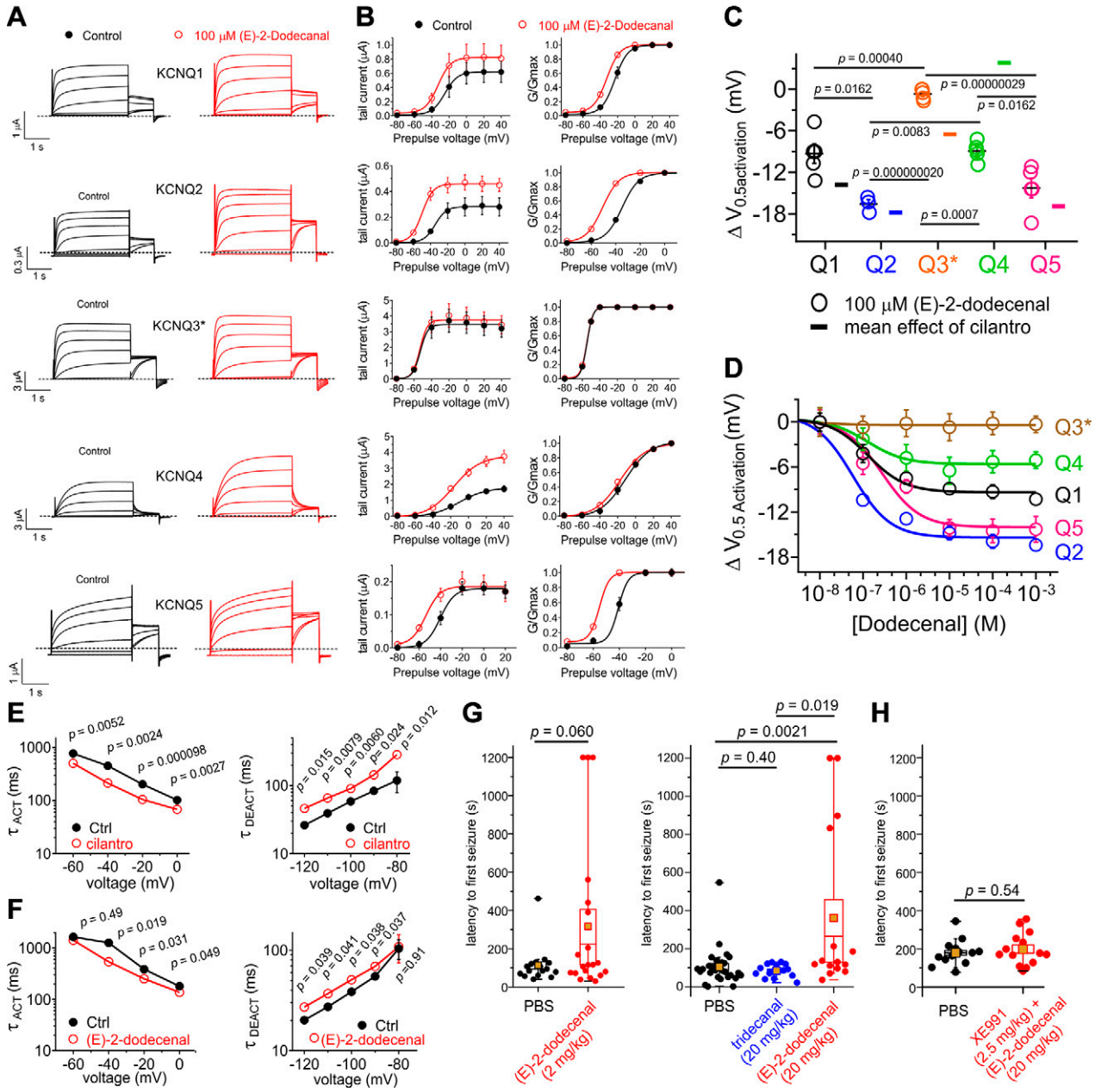

Figure 4. (E)-2-dodecenal and cilantro extract exhibit similar KCNQ isoform selectivity and anticonvulsant effects. All error bars indicate SEM. *A*) Mean TEVC current traces showing effects of (E)-2-dodecenal (100 μM) on homomeric KCNQ channels expressed in *Xenopus* oocytes; $n = 5$ except for KCNQ2 ($n = 3$). *B*) Mean tail current (left) and normalized tail currents (G/G_{max}) (right) *vs.* prepulse voltage relationships for the traces as in *A*; $n = 5$ except for KCNQ2 ($n = 3$). *C*) Mean $\Delta V_{0.5\ activation}$ induced by (E)-2-dodecenal (100 μM) (scatter plot) *vs.* mean effects of 1% cilantro extract (single bars indicate means from Figs. 1 and 2) for the homomeric KCNQ isoforms indicated; $n = 5$ except for KCNQ2 ($n = 3$). *D*) (E)-2-dodecenal dose responses for homomeric KCNQ1–5 channels ($n = 3$–5). *E*, *F*) Comparison of effects of 1% cilantro extract (*E*) *vs.* (E)-2-dodecenal (100 μM) (*F*) on KCNQ2/3 activation and deactivation rate *vs.* voltage; $n = 6$. *G*) Mean latency to first PTZ-induced seizure for mice preinjected with PBS ($n = 16$) *vs.* (E)-2-dodecenal (2 mg/kg) ($n = 20$) (left) or PBS ($n = 29$) *vs.* tridecanal (20 mg/kg) ($n = 15$) or (E)-2-dodecenal (20 mg/kg) ($n = 15$) (right). Statistical analysis was by 2-way ANOVA corrected for multiple comparisons. Gold squares = mean values. *H*) Mean latency to first PTZ-induced seizure for mice preinjected with PBS ($n = 14$) or 20 mg/kg (E)-2-dodecenal + 2.5 mg/kg XE991 ($n = 13$). Statistical analysis was by 2-way ANOVA.

relatively low current magnitude; therefore, instead, we examined the effects of single mutants of KCNQ2 and KCNQ3 in the context of KCNQ2/3 complexes. Each of the S5 W mutants (KCNQ2-W236 and KCNQ3-W265) exerted a similar effect on the maximal shift in KCNQ2/3 $V_{0.5\ activation}$ induced by (E)-2-dodecenal, reducing this to −9 mV, a value intermediate between that of wild-type and WL/WL double-mutant KCNQ2/3 channels (**Fig. 6*A*–*C***). Each of the S5 W mutants also reduced the potency of (E)-2-dodecenal compared with wild-type KCNQ2/3, but the KCNQ2-W236L mutation reduced potency 20-fold more than did the KCNQ3-W265L

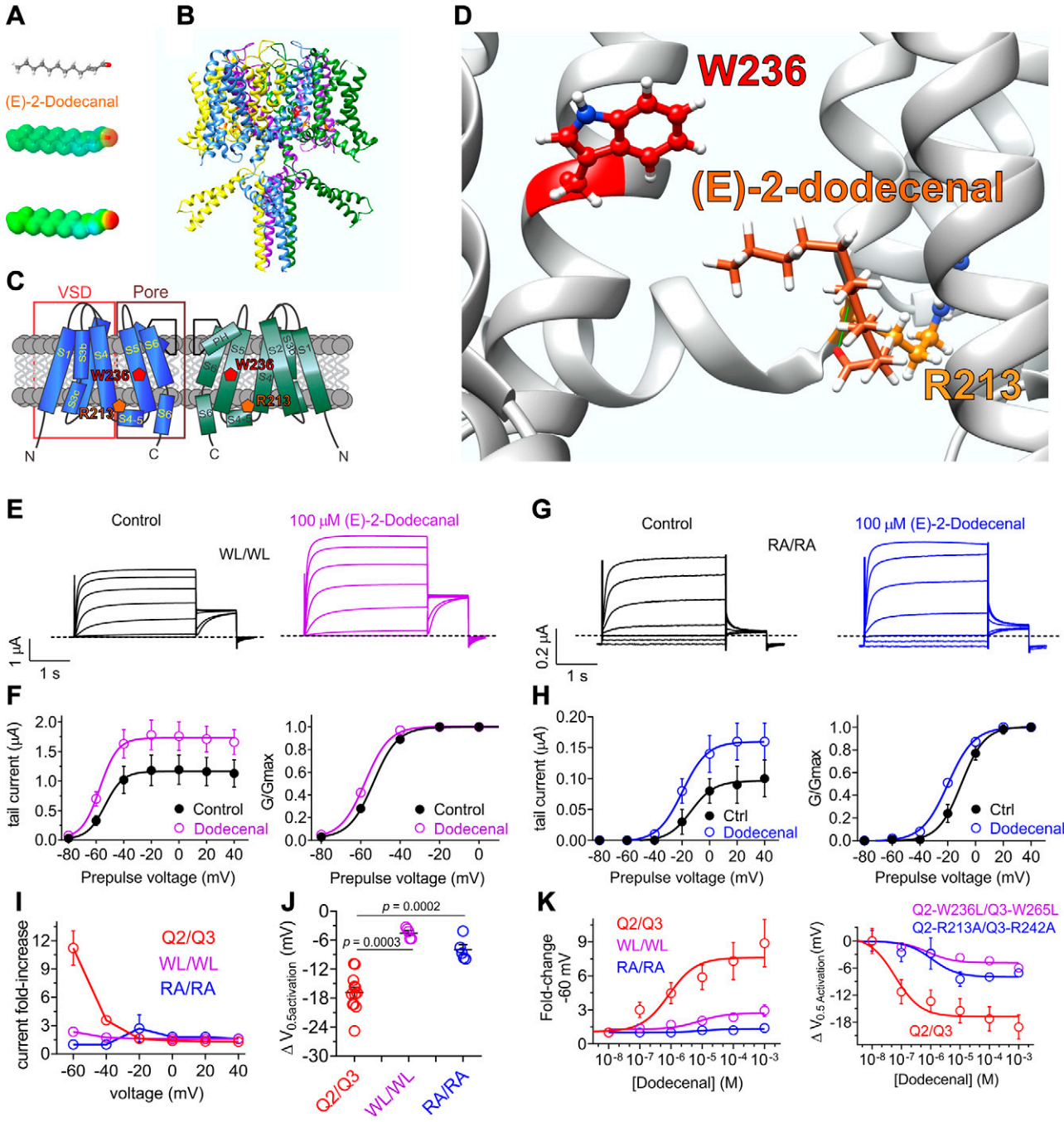

Figure 5. KCNQ2/3 activation by (E)-2-dodecenal requires a conserved S5 tryptophan and S4–5 arginine. All error bars indicate SEM. *A*) (E)-2-dodecenal chemical structure (upper and center) and electrostatic surface potentials (red, electron-dense; blue, electron-poor; green, neutral) (lower and center) calculated and plotted using Jmol. *B*) Chimeric KCNQ1/KCNQ2 structural model (orange, KCNQ2-R213; red, KCNQ2-W236). *C*) Topological representation of KCNQ5 showing 2 of the 4 subunits, without domain swapping for clarity. *Pentagons*, approximate position of KCNQ2-R213 (orange) and KCNQ2-W236 (red); *D*) View of the (E)-2-dodecenal binding site in KCNQ2 predicted by SwissDock. Green line, predicted H-bond. *E*) Mean TEVC current traces showing effects of (E)-2-dodecenal (100 μM) on KCNQ2-W236L/KCNQ3-W265L (WL/WL) channels expressed in *Xenopus* oocytes ($n = 5–6$). *F*) Mean tail current (left) and mean normalized tail currents (G/G_{max}) (right) *vs.* prepulse voltage relationships for the traces as in *E* ($n = 5–6$). *G*) Mean TEVC current traces showing effects of (E)-2-dodecenal (100 μM) on KCNQ2-R213A/KCNQ3-R242 (RA/RA) channels expressed in *Xenopus* oocytes ($n = 5–6$). *H*) Mean tail current (left) and mean normalized tail currents (G/G_{max}) (right) *vs.* prepulse voltage relationships for the traces as in *G* ($n = 5–6$). *I*) Current-fold increase *vs.* voltage in response to (E)-2-dodecenal (100 μM) of wild-type (Q2/Q3), WL/WL, and RA/RA KCNQ2/3 channels ($n = 5–6$). *J*) Scatter plot showing $\Delta V_{0.5\ activation}$ in response to (E)-2-dodecenal (100 μM) of wild-type (Q2/Q3), WL/WL and RA/RA KCNQ2/3 channels ($n = 5–6$). *K*) (E)-2-dodecenal dose response calculated from fold increase in current at −60 mV (left) and $\Delta V_{0.5\ activation}$ (right) for wild-type (Q2/Q3), WL/WL, and RA/RA KCNQ2/3 channels; $n = 5–6$.

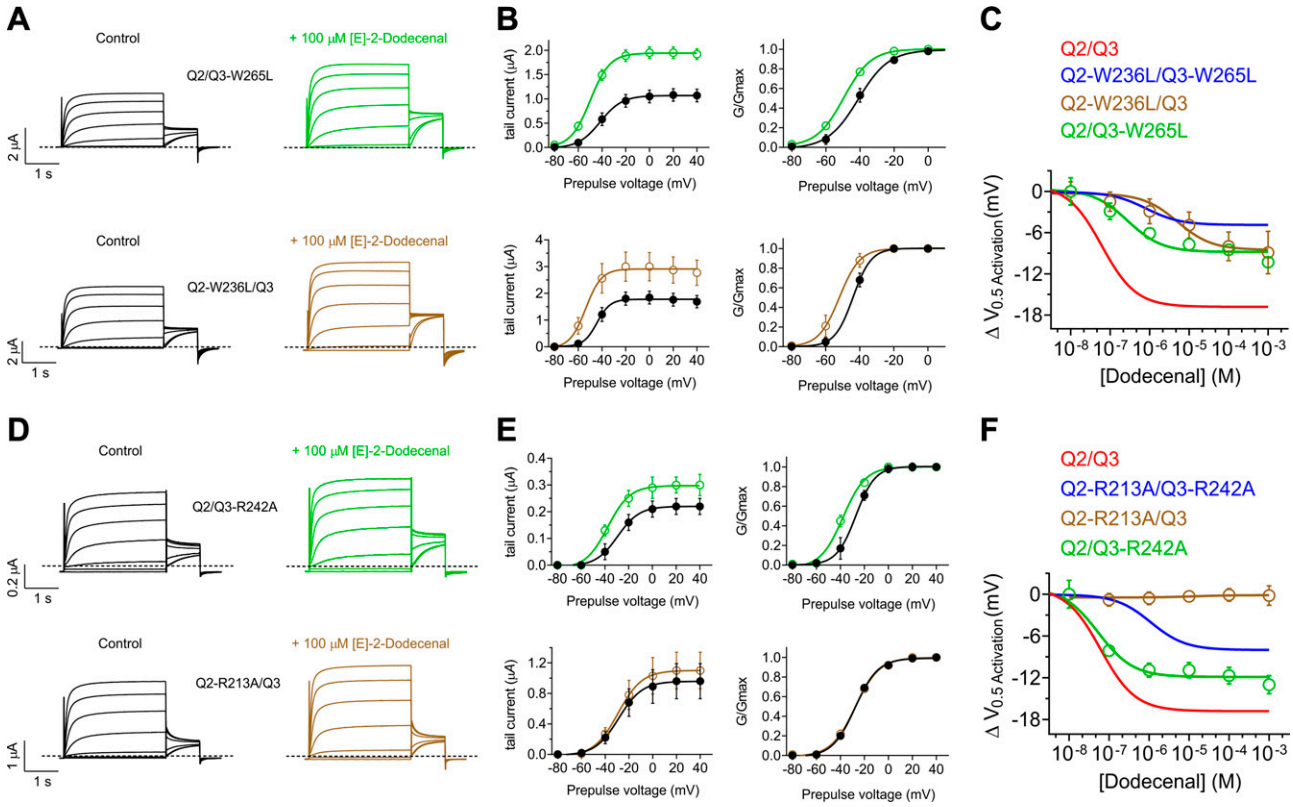

Figure 6. KCNQ2-R213 is essential for KCNQ2/3 activation by (E)-2-dodecenal. All error bars indicate SEM. *A*) Mean TEVC current traces showing effects of (E)-2-dodecenal (100 μM) on KCNQ2/KCNQ3-W265L (upper) and KCNQ2-W236L/KCNQ3 (lower) channels expressed in *Xenopus* oocytes (n = 5–6). *B*) Mean tail currents (left) and mean normalized tail currents (G/G_{max}) (right) *vs.* prepulse voltage relationships for the traces as in *A* (n = 5–6). *C*) (E)-2-dodecenal dose response calculated from $\Delta V_{0.5\ activation}$ for wild-type, double-mutant (from Fig. 5), and single-mutant KCNQ2/3 channels as indicated; n = 5–6. *D*) Mean TEVC current traces showing effects of (E)-2-dodecenal (100 μM) on KCNQ2/KCNQ3-R242A (upper) and KCNQ2-R213A/KCNQ3 (lower) channels expressed in *Xenopus* oocytes (n = 5). *E*) Mean tail currents (left) and mean normalized tail currents (G/G_{max}) (right) *vs.* prepulse voltage relationships for the traces as in *D* (n = 5). *F*) (E)-2-dodecenal dose response calculated from $\Delta V_{0.5\ activation}$ for wild-type, double-mutant (from Fig. 5), and single-mutant KCNQ2/3 channels as indicated (n = 5).

mutation—from an EC_{50} of 60 ± 20 nM (wild type) to 5.07 ± 0.5 μM (KCNQ2-W236L/KCNQ3) *vs.* 270 ± 20 nM (KCNQ2/KCNQ3-W265L) (Fig. 6*A–C* and Supplemental Tables S24, S33, and S34).

In contrast, the KCNQ2-R213A mutation rendered KCNQ2/3 channels completely insensitive to (E)-2-dodecenal, whereas the equivalent KCNQ3-R242A mutant channel responded to (E)-2-dodecenal almost as much as wild-type KCNQ2/3 (similar potency, slightly lower efficacy) (Fig. 6*D–F* and Supplemental Tables S24, S35, and S36).

Overall, the W and R mutant data are consistent, with the R being more influential than the W in terms of (E)-2-dodecenal binding/activation and also with KCNQ2 channels being more sensitive than KCNQ3 to (E)-2-dodecenal. Because homomeric KCNQ3* is insensitive to (E)-2-dodecenal (Fig. 4), one might ask why the KCNQ3 mutants have any effect at all. However, the Kv channel complexes exhibit "domain swapping," whereby the S4 of 1 subunit aligns with the pore module of the adjoining subunit, and the binding pocket between the S5 W and the S4-5 R must therefore actually form from 2 adjoining subunits. Therefore, if as expected in KCNQ2/3 complexes the subunits alternate isoforms, the KCNQ2 W would form a binding site together with the KCNQ3 R, and *vice versa*, and thus a mutation in KCNQ3 would be predicted to disrupt a drug binding site formed in conjunction with the more sensitive KCNQ2 subunit.

These data support the docking predictions and suggest that (E)-2-dodecenal activates KCNQ2/3 channels by binding in a site spanning S5 and the S4-5 linker, specifically between (KCNQ2 numbering) W236 and R213, with KCNQ2-R213 being the most influential residue tested.

KCNE1 impacts the KCNQ1 (E)-2-dodecenal binding site

KCNQ1 lacks the KCNQ2-W236 equivalent but possesses the KCNQ2-R213 equivalent (R243 in human KCNQ1); therefore, we also investigated the mechanism of (E)-2-dodecenal binding in KCNQ1 channels and how this might be impacted by coassembly with KCNE regulatory subunits. Although (E)-2-dodecenal had minimal effects on KCNQ1/KCNE2 (Supplemental Fig. S1*E*, *F* and Supplemental Table S37), cilantro (Fig. 2) and (E)-2-dodecenal (Supplemental Fig. S1*G*, *H*) each activated KCNQ1/KCNE3 across the voltage range. Given that the minimal voltage dependence of KCNQ1/KCNE3 complexes

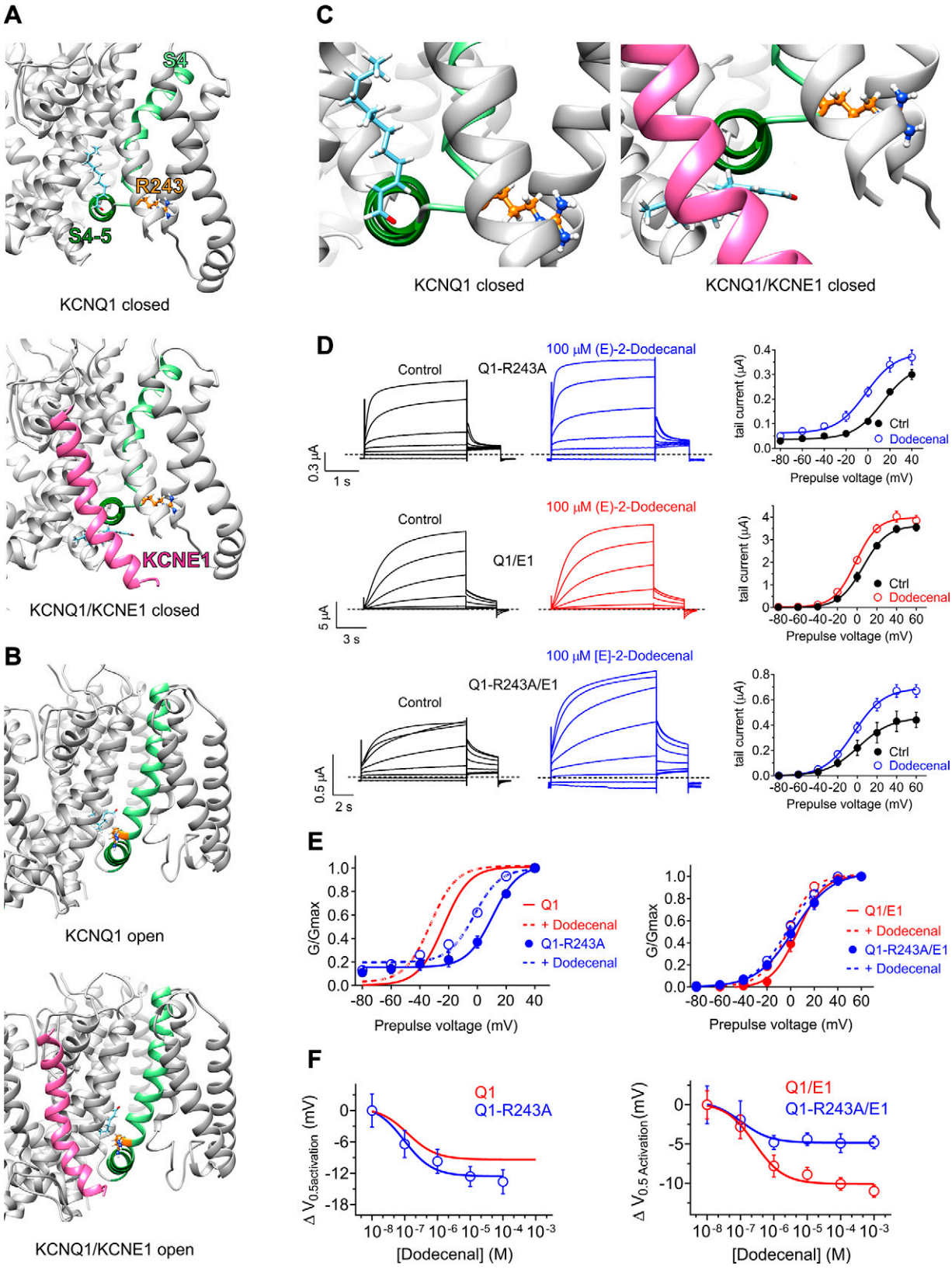

Figure 7. KCNE1 impinges on the KCNQ1 (E)-2-dodecenal binding site. All error bars indicate SEM. For structural models: Pink, KCNE1; pale green, KCNQ1-S4; forest green, KCNQ1-S4/5 linker; orange, KCNQ1-R243; pale blue, (E)-2-dodecenal. *A*) View of the (E)-2-dodecenal binding site predicted by SwissDock in the KCNQ1 (upper) and KCNQ1/KCNE1 (lower) closed-state models. *B*) View of the (E)-2-dodecenal binding site predicted by SwissDock in the KCNQ1 (upper) and KCNQ1/KCNE1 (lower) open-state models. *C*) Close-up view of the (E)-2-dodecenal binding site predicted by SwissDock (from *A*), highlighting the predicted KCNE1-induced shift in the (E)-2-dodecenal binding pose in the closed-state models. *D*) Mean TEVC current traces

(*continued on next page*)

stymies quantification of effects, we focused on KCNQ1/KCNE1 here, which, as we showed earlier, was activated by cilantro (Fig. 2).

We first performed *in silico* docking to predict possible binding sites of (E)-2-dodecenal to KCNQ1 and KCNQ1/KCNE1 channels, using coordinates from previously published closed- and open-state models (29) (**Fig. 7*A, B***). This revealed a possible binding site for (E)-2-dodecenal close to the KCNQ1 S4-5 linker and in the vicinity of R243, in the closed state (Fig. 7*A*). Interestingly, (E)-2-dodecenal was predicted to bind proximal to KCNE1, which altered the position of (E)-2-dodecenal in docking simulations predicting binding proximal to R243 (Fig. 7*A, C*). In the open state, KCNE1 did not alter the predicted binding site of (E)-2-dodecenal (Fig. 7*B*).

We tested the predicted influence of KCNE1 by comparing effects on (E)-2-dodecenal binding of an R243A mutation in KCNQ1 *vs.* KCNQ1/KCNE1 channels using TEVC (Fig. 7*D*). In homomeric KCNQ1, the R243A mutation positive-shifted $V_{0.5\ activation}$ and introduced a minor constitutively active current component, as we previously reported (42). Moreover, the mutation slightly increased (E)-2-dodecenal efficacy for KCNQ1 activation (Fig. 7*E, F* and Supplemental Tables S24 and S38). In contrast, the R243A mutation had only minor effects on KCNQ1-KCNE1 $V_{0.5\ activation}$, as we also previously reported (42). Wild-type KCNQ1-KCNE1 was >2-fold less sensitive than KCNQ1 to (E)-2-dodecenal but with similar efficacy (Fig. 7*F* and Supplemental Table S24). In contrast to mutant effects on homomeric KCNQ1, the R243A mutation reduced (E)-2-dodecenal efficacy 2-fold in KCNQ1/KCNE1 channels while more than doubling the sensitivity (Fig. 7*F* and Supplemental Tables S24, S39, and S40). The results suggest that both KCNQ1-R243 and KCNE1 influence (E)-2-dodecenal binding.

DISCUSSION

Our findings demonstrate for the first time a specific molecular basis for the anticonvulsant effects of cilantro and show that this widely and frequently used food plant is highly effective at activating multiple isoforms within a clinically prominent family of human Kv channels. Aside from its noted anticonvulsant action, cilantro has historically been used to treat hypertension and digestive disorders and has reported anti-inflammatory, antibacterial, analgesic, and other potentially therapeutic properties (8). The tissue expression of cilantro-sensitive KCNQs suggests their activation could contribute to many of the reported therapeutic effects of cilantro.

The activity profile of (E)-2-dodecenal in delaying seizure onset is remarkably similar to that observed for cilantro extract in a previous study employing PTZ-induced seizures in rats (36). We observed anticonvulsant activity at 2 mg/kg (E)-2-dodecenal, equivalent to 11 μM, a concentration at which the (E)-2-dodecenal dose response curve shifts with respect to shift in the $V_{0.5\ activation}$ of KCNQ2/3 saturates (Fig. 5*K*, right). Coupled with the highly similar KCNQ activation profiles of (E)-2-dodecenal and whole cilantro extract, this provides strong evidence for (E)-2-dodecenal activation of KCNQs (and likely primarily KCNQ2/3 heteromers) being the molecular basis for the anticonvulsant effects of cilantro.

Furthermore, (E)-2-dodecenal, also known as eryngial, is the primary component of the essential oil produced from leaves of *Eryngium foetidum*, (culantro or Mexican coriander), a plant also used extensively as a food across Asia, Africa, and the Caribbean and utilized in folk medicine as an anticonvulsant and hypotensive, among other applications (43). Interestingly, the neuronally expressed (44) channel KCNQ5 is also highly expressed in the vasculature (45, 46), and its activation reduces vascular tone, potentially reducing blood pressure (20). Here, we found cilantro extract and specifically (E)-2-dodecenal, previously identified as the predominant component of cilantro leaf oil (35), to be a highly efficacious KCNQ5 activator, suggesting a possible molecular basis contributing to the historical use of cilantro and culantro as folk hypotensives, an application that was recently verified using cilantro crude extract in animal studies (47). KCNQ5 gene variants (48) and aberrant splicing (49) that impair its function cause epilepsy (and severe intellectual disability), suggesting its activation could also contribute to the anticonvulsant action of cilantro [and (E)-2-dodecenal].

We also found that coassembly with KCNE1 influenced the cilantro and (E)-2-dodecenal sensitivity of KCNQ1. KCNQ1-KCNE1 complexes generate the I_{Ks} current that helps to repolarize ventricular cardiomyocytes. I_{Ks} is down-regulated in heart failure, which is suggested to contribute to increased risk of ventricular fibrillation in heart failure (50). It is fascinating, then, that cilantro extract was recently found to improve left ventricular function in heart failure (51). KCNQ1 also forms complexes with KCNE subunits across along the gastrointestinal tract—with KCNE2 (in the stomach) and KCNE3 (in the colon, intestine, and duodenum) (21). Here we found that KCNQ1-KCNE3 channel activity is potentiated by cilantro and by (E)-2-dodecenal. Stimulation of KCNQ1-KCNE3 activity by cilantro lower in the gastrointestinal tract would be expected to increase cAMP-stimulated Cl^- secretion (34) and thus promote digestion and buffer the luminal environment to protect against damage from gastric acid effluent (52). Activation of KCNQ5 by cilantro could also contribute to its gut stimulatory properties, as KCNQ5 is also expressed in gastrointestinal smooth

(left) and mean tail current *vs.* prepulse voltage relationships (right) showing effects of (E)-2-dodecenal (100 μM) on channels indicated (n = 5). *E*) Mean normalized tail current (G/G_{max}) *vs.* prepulse voltage relationships showing effects of (E)-2-dodecenal (100 μM) (dashed lines) on the voltage dependence of activation of wild-type and R243A KCNQ1 (Q1) alone (left) or with KCNE1 (E1) (right); n = 5. Wild-type KCNQ1 data are from Fig 4*B*. *F*) (E)-2-dodecenal dose response calculated from $\Delta V_{0.5\ activation}$ for wild-type and R243A KCNQ1 (Q1) alone (left) or with KCNE1 (E1) (right); n = 5. Wild-type KCNQ1 data are from Fig. 4*B*.

muscle (53), and its activation might therefore relax muscle, potentially being therapeutic in gastric motility disorders such as diabetic gastroparesis.

The KCNQ activation profile of (E)-2-dodecenal bears both similarities and differences to that of other KCNQ openers. We recently found that mallotoxin, from the shrub *Mallotus oppositifolius* that is used in African folk medicine, also activates KCNQ1-5 homomers, prefers KCNQ2 over KCNQ3, and in docking simulations binds in a pose reminiscent to that predicted for (E)-2-dodecenal, between (KCNQ2 numbering) R213 and W236. As for (E)-2-dodecenal (Fig. 5), the importance for mallotoxin binding of R213 outweighs that of W236, as determined using site-directed mutagenesis and TEVC of wild-type and mutant KCNQ2/3 channels (11, 41). Interestingly, mutation of human KCNQ2-R213 is associated with benign familial neonatal convulsions (54), and the residue represents a hinge point between the pore module and the VSD.

Although retigabine does not activate KCNQ1, because it lacks the equivalent S5 tryptophan (39), (E)-2-dodecenal and mallotoxin both do. Although the KCNQ family–conserved arginine at the voltage sensor foot (R243 in KCNQ1) was essential for mallotoxin binding to KCNQ2/3, KCNQ1, and KCNQ1/KCNE1 channels (41), an arginine at position 243 was not essential for (E)-2-dodecenal activation of KCNQ1 or KCNQ1/KCNE1. However, docking simulations and shifts in potency and efficacy resulting from R243A mutation suggest (E)-2-dodecenal binds somewhat proximal to R243 and the S4-5 linker (Fig. 7), placing it in a location where its binding conformation can be influenced by KCNE1 (29). Although (E)-2-dodecenal shares with mallotoxin a preference for KCNQ2 and KCNQ5 over KCNQ3 and KCNQ4 (41), both botanical compounds (which incidentally share negligible structural similarity with one another) offer a different activity profile to typical synthetic KCNQ openers. Thus, retigabine and ML213 slightly favor KCNQ3 over KCNQ2, 4, and 5. ICA-069673 is a 20-fold more activator of KCNQ2/3 *vs.* KCNQ3/5 activation (55), but also strongly activates KCNQ4 (56); in contrast, ICA-27243 is >20-fold more potent at opening KCNQ2/3 *vs.* KCNQ4 (57).

(E)-2-dodecenal is a *trans*-2,3-unsaturated fatty aldehyde that possesses a carbonyl oxygen at one end, which is predicted to provide a strong negative electrostatic surface potential in that region of the molecule (Fig. 3*A*). This chemical property is required for binding of retigabine to the S5 tryptophan of KCNQ channels (W236 in KCNQ2); yet, in our docking simulations, the carbonyl oxygen instead participated in hydrogen bonding with KCNQ2-R213 and the uncharged end faced W236. Furthermore, several cilantro leaf components highly similar to (E)-2-dodecenal, including 10, 11, and [^{13}C] species each containing the similarly positioned and negative surface-charged carbonyl oxygen, were completely inactive against KCNQ2/3 (at 100 μM). Whether the chain length of (E)-2-dodecenal is crucial to it accessing the KCNQ binding site *vs.* it being the perfect size to activate once inside the binding site, we do not yet know, but the chemical selectivity for KCNQ2/3 opening activity within this family of *trans*-2-alkenals is remarkable. In contrast, (E)-2-dodecenal is also an effective antibiotic (probably contributing to the antibacterial effects of cilantro), but in this case, bactericidal potency increases with each CH_2 group up to (E)-2-dodecenal and the bactericidal activity EC_{50} is >30 μM. The bactericidal activity reflects a nonspecific (but nevertheless effective) activity probably stemming from the nonionic surfactant properties of (E)-2-dodecenal (58).

In addition to the widespread use of cilantro in cooking and as an herbal medicine, (E)-2-dodecenal itself is in broad use as a food flavoring and to provide citrus notes to cosmetics, perfumes, soaps, detergents, shampoos, and candles (59). Our mouse seizure studies suggest it readily accesses the brain, and it is likely that its consumption as a food or herbal medicine (in cilantro) or as an added food flavoring would result in KCNQ-active levels in the human body; we found the 1% cilantro extract an efficacious KCNQ activator, and (E)-2-dodecenal itself showed greater than half-maximal opening effects on KCNQ2/3 at 100 nM (>10 mV shift at this concentration) (EC_{50}, 60 ± 20 nM). We anticipate that its activity on KCNQ channels contributes significantly to the broad therapeutic spectrum attributed to cilantro, which has persisted as a folk medicine for thousands of years throughout and perhaps predating human recorded history. FJ

ACKNOWLEDGMENTS

The authors are grateful to Angele De Silva (University of California–Irvine) for generating mutant channel constructs, and to Bo Abbott for botanical photography. This study was supported by the U.S. National Institutes of Health (NIH) National Institute of General Medical Sciences (Grants GM115189 and GM130377 to G.W.A.) and NIH National Institute of Neurological Disorders and Stroke (Grant NS107671 to G.W.A.). The authors declare no conflicts of interest.

AUTHOR CONTRIBUTIONS

R. W. Manville performed the oocyte experiments and analyses, prepared solutions and syringes for seizure studies, prepared most of the figure panels, and edited the manuscript; and G. W. Abbott prepared cilantro extracts, performed *in silico* structural analyses, quantified seizure latencies, wrote the manuscript, and helped prepare the figures.

REFERENCES

1. Inskeep, R. R. (1969) Health hazards and healing in antiquity. *S. Afr. Archaeol. Bull.* **24**, 21–29
2. Hardy, K., Buckley, S., Collins, M. J., Estalrrich, A., Brothwell, D., Copeland, L., García-Tabernero, A., García-Vargas, S., de la Rasilla, M., Lalueza-Fox, C., Huguet, R., Bastir, M., Santamaría, D., Madella, M., Wilson, J., Cortés, A. F., and Rosas, A. (2012) Neanderthal medics? Evidence for food, cooking, and medicinal plants entrapped in dental calculus. *Naturwissenschaften* **99**, 617–626
3. Weyrich, L. S., Duchene, S., Soubrier, J., Arriola, L., Llamas, B., Breen, J., Morris, A. G., Alt, K. W., Caramelli, D., Dresely, V., Farrell, M., Farrer, A. G., Francken, M., Gully, N., Haak, W., Hardy, K., Harvati, K., Held, P., Holmes, E. C., Kaidonis, J., Lalueza-Fox, C., de la Rasilla, M., Rosas, A., Semal, P., Soltysiak, A., Townsend, G., Usai, D., Wahl, J., Huson, D. H., Dobney, K., and Cooper, A. (2017) Neanderthal

behaviour, diet, and disease inferred from ancient DNA in dental calculus. *Nature* **544**, 357–361
4. Melamed, Y., Kislev, M. E., Geffen, E., Lev-Yadun, S., and Goren-Inbar, N. (2016) The plant component of an Acheulian diet at Gesher Benot Ya'aqov, Israel. *Proc. Natl. Acad. Sci. USA* **113**, 14674–14679
5. Hoffmann, D. (2003) *Medical Herbalism: The Science and Practice of Herbal Medicine*, Healing Arts Press, Rochester, VT, USA
6. Moerman, D. E. (2009) *Native American Medicinal Plants*, Timber Press, Portland, OR, USA
7. Cumo, C. (2013) *Encyclopedia of Cultivated Plants: From Acacia to Zinnia*, ABC-CLIO, Santa Barbara, CA, USA
8. Sahib, N. G., Anwar, F., Gilani, A. H., Hamid, A. A., Saari, N., and Alkharfy, K. M. (2013) Coriander (Coriandrum sativum L.): a potential source of high-value components for functional foods and nutraceuticals–a review. *Phytother. Res.* **27**, 1439–1456
9. Main, M. J., Cryan, J. E., Dupere, J. R., Cox, B., Clare, J. J., and Burbidge, S. A. (2000) Modulation of KCNQ2/3 potassium channels by the novel anticonvulsant retigabine. *Mol. Pharmacol.* **58**, 253–262
10. Manville, R. W., and Abbott, G. W. (2018) Gabapentin is a potent activator of KCNQ3 and KCNQ5 potassium channels. *Mol. Pharmacol.* **94**, 1155–1163
11. Manville, R. W., and Abbott, G. W. (2018) Ancient and modern anticonvulsants act synergistically in a KCNQ potassium channel binding pocket. *Nat. Commun.* **9**, 3845
12. Manville, R. W., Papanikolaou, M., and Abbott, G. W. (2018) Direct neurotransmitter activation of voltage-gated potassium channels. *Nat. Commun.* **9**, 1847
13. Wickenden, A. D., Yu, W., Zou, A., Jegla, T., and Wagoner, P. K. (2000) Retigabine, a novel anti-convulsant, enhances activation of KCNQ2/Q3 potassium channels. *Mol. Pharmacol.* **58**, 591–600
14. Tatulian, L., Delmas, P., Abogadie, F. C., and Brown, D. A. (2001) Activation of expressed KCNQ potassium currents and native neuronal M-type potassium currents by the anti-convulsant drug retigabine. *J. Neurosci.* **21**, 5535–5545
15. Biervert, C., Schroeder, B. C., Kubisch, C., Berkovic, S. F., Propping, P., Jentsch, T. J., and Steinlein, O. K. (1998) A potassium channel mutation in neonatal human epilepsy. *Science* **279**, 403–406
16. Klinger, F., Gould, G., Boehm, S., and Shapiro, M. S. (2011) Distribution of M-channel subunits KCNQ2 and KCNQ3 in rat hippocampus. *Neuroimage* **58**, 761–769
17. Singh, N. A., Charlier, C., Stauffer, D., DuPont, B. R., Leach, R. J., Melis, R., Ronen, G. M., Bjerre, I., Quattlebaum, T., Murphy, J. V., McHarg, M. L., Gagnon, D., Rosales, T. O., Peiffer, A., Anderson, V. E., and Leppert, M. (1998) A novel potassium channel gene, KCNQ2, is mutated in an inherited epilepsy of newborns. *Nat. Genet.* **18**, 25–29
18. Tzingounis, A. V., Heidenreich, M., Kharkovets, T., Spitzmaul, G., Jensen, H. S., Nicoll, R. A., and Jentsch, T. J. (2010) The KCNQ5 potassium channel mediates a component of the afterhyperpolarization current in mouse hippocampus. *Proc. Natl. Acad. Sci. USA* **107**, 10232–10237
19. Wang, H. S., Pan, Z., Shi, W., Brown, B. S., Wymore, R. S., Cohen, I. S., Dixon, J. E., and McKinnon, D. (1998) KCNQ2 and KCNQ3 potassium channel subunits: molecular correlates of the M-channel. *Science* **282**, 1890–1893
20. Yeung, S. Y., Pucovský, V., Moffatt, J. D., Saldanha, L., Schwake, M., Ohya, S., and Greenwood, I. A. (2007) Molecular expression and pharmacological identification of a role for K(v)7 channels in murine vascular reactivity. *Br. J. Pharmacol.* **151**, 758–770
21. Abbott, G. W. (2014) Biology of the KCNQ1 potassium channel. *New J. Sci.* **2014**, 26
22. Kubisch, C., Schroeder, B. C., Friedrich, T., Lütjohann, B., El-Amraoui, A., Marlin, S., Petit, C., and Jentsch, T. J. (1999) KCNQ4, a novel potassium channel expressed in sensory outer hair cells, is mutated in dominant deafness. *Cell* **96**, 437–446
23. Neyroud, N., Tesson, F., Denjoy, I., Leibovici, M., Donger, C., Barhanin, J., Fauré, S., Gary, F., Coumel, P., Petit, C., Schwartz, K., and Guicheney, P. (1997) A novel mutation in the potassium channel gene KVLQT1 causes the Jervell and Lange-Nielsen cardioauditory syndrome. *Nat. Genet.* **15**, 186–189
24. Sun, J., and MacKinnon, R. (2017) Cryo-EM structure of a KCNQ1/CaM complex reveals insights into congenital long QT syndrome. *Cell* **169**, 1042–1050.e9
25. Van Gunsteren, W. F. (1996) *Biomolecular Simulation: The GROMOS96 Manual and User Guide*, Biomos, Zürich Switzerland
26. Johansson, M. U., Zoete, V., Michielin, O., and Guex, N. (2012) Defining and searching for structural motifs using DeepView/Swiss-PdbViewer. *BMC Bioinformatics* **13**, 173
27. Grosdidier, A., Zoete, V., and Michielin, O. (2011) SwissDock, a protein-small molecule docking web service based on EADock DSS. *Nucleic Acids Res.* **39** (Suppl), W270–W277
28. Grosdidier, A., Zoete, V., and Michielin, O. (2011) Fast docking using the CHARMM force field with EADock DSS. *J. Comput. Chem.* **32**, 2149–2159
29. Kang, C., Tian, C., Sönnichsen, F. D., Smith, J. A., Meiler, J., George, A. L., Jr., Vanoye, C. G., Kim, H. J., and Sanders, C. R. (2008) Structure of KCNE1 and implications for how it modulates the KCNQ1 potassium channel. *Biochemistry* **47**, 7999–8006
30. Abbott, G. W., Tai, K. K., Neverisky, D. L., Hansler, A., Hu, Z., Roepke, T. K., Lerner, D. J., Chen, Q., Liu, L., Zupan, B., Toth, M., Haynes, R., Huang, X., Demirbas, D., Buccafusca, R., Gross, S. S., Kanda, V. A., and Berry, G. T. (2014) KCNQ1, KCNE2, and Na+-coupled solute transporters form reciprocally regulating complexes that affect neuronal excitability. *Sci. Signal.* **7**, ra22
31. Etxeberria, A., Santana-Castro, I., Regalado, M. P., Aivar, P., and Villarroel, A. (2004) Three mechanisms underlie KCNQ2/3 heteromeric potassium M-channel potentiation. *J. Neurosci.* **24**, 9146–9152
32. Tyson, J., Tranebjaerg, L., Bellman, S., Wren, C., Taylor, J. F., Bathen, J., Aslaksen, B., Sørland, S. J., Lund, O., Malcolm, S., Pembrey, M., Bhattacharya, S., and Bitner-Glindzicz, M. (1997) IsK and KvLQT1: mutation in either of the two subunits of the slow component of the delayed rectifier potassium channel can cause Jervell and Lange-Nielsen syndrome. *Hum. Mol. Genet.* **6**, 2179–2185
33. Vetter, D. E., Mann, J. R., Wangemann, P., Liu, J., McLaughlin, K. J., Lesage, F., Marcus, D. C., Lazdunski, M., Heinemann, S. F., and Barhanin, J. (1996) Inner ear defects induced by null mutation of the isk gene. *Neuron* **17**, 1251–1264
34. Schroeder, B. C., Waldegger, S., Fehr, S., Bleich, M., Warth, R., Greger, R., and Jentsch, T. J. (2000) A constitutively open potassium channel formed by KCNQ1 and KCNE3. *Nature* **403**, 196–199
35. Potter, T. L. (1996) Essential oil composition of cilantro. *J. Agric. Food Chem.* **44**, 1824–1826
36. Karami, R., Hosseini, M., Mohammadpour, T., Ghorbani, A., Sadeghnia, H. R., Rakhshandeh, H., Vafaee, F., and Esmaeilizadeh, M. (2015) Effects of hydroalcoholic extract of Coriandrum sativum on oxidative damage in pentylenetetrazole-induced seizures in rats. *Iran. J. Neurol.* **14**, 59–66
37. Gilling, M., Rasmussen, H. B., Calloe, K., Sequeira, A. F., Baretto, M., Oliveira, G., Almeida, J., Lauritsen, M. B., Ullmann, R., Boonen, S. E., Brondum-Nielsen, K., Kalscheuer, V. M., Tümer, Z., Vicente, A. M., Schmitt, N., and Tommerup, N. (2013) Dysfunction of the heteromeric KV7.3/KV7.5 potassium channel is associated with autism spectrum disorders. *Front. Genet.* **4**, 54
38. Lerche, C., Scherer, C. R., Seebohm, G., Derst, C., Wei, A. D., Busch, A. E., and Steinmeyer, K. (2000) Molecular cloning and functional expression of KCNQ5, a potassium channel subunit that may contribute to neuronal M-current diversity. *J. Biol. Chem.* **275**, 22395–22400
39. Schenzer, A., Friedrich, T., Pusch, M., Saftig, P., Jentsch, T. J., Grötzinger, J., and Schwake, M. (2005) Molecular determinants of KCNQ (Kv7) K+ channel sensitivity to the anticonvulsant retigabine. *J. Neurosci.* **25**, 5051–5060
40. Kim, R. Y., Yau, M. C., Galpin, J. D., Seebohm, G., Ahern, C. A., Pless, S. A., and Kurata, H. T. (2015) Atomic basis for therapeutic activation of neuronal potassium channels. *Nat. Commun.* **6**, 8116
41. De Silva, A. M., Manville, R. W., and Abbott, G. W. (2018) Deconstruction of an African folk medicine uncovers a novel molecular strategy for therapeutic potassium channel activation. *Sci. Adv.* **4**, eaav0824
42. Panaghie, G., and Abbott, G. W. (2007) The role of S4 charges in voltage-dependent and voltage-independent KCNQ1 potassium channel complexes. *J. Gen. Physiol.* **129**, 121–133
43. Paul, J. H., Seaforth, C. E., and Tikasingh, T. (2011) Eryngium foetidum L.: a review. *Fitoterapia* **82**, 302–308
44. Schroeder, B. C., Hechenberger, M., Weinreich, F., Kubisch, C., and Jentsch, T. J. (2000) KCNQ5, a novel potassium channel broadly expressed in brain, mediates M-type currents. *J. Biol. Chem.* **275**, 24089–24095
45. Mackie, A. R., Brueggemann, L. I., Henderson, K. K., Shiels, A. J., Cribbs, L. L., Scrogin, K. E., and Byron, K. L. (2008) Vascular KCNQ potassium channels as novel targets for the control of mesenteric artery constriction by vasopressin, based on studies in single cells,

pressurized arteries, and in vivo measurements of mesenteric vascular resistance. *J. Pharmacol. Exp. Ther.* **325**, 475–483
46. Yeung, S., Schwake, M., Pucovský, V., and Greenwood, Ia. (2008) Bimodal effects of the Kv7 channel activator retigabine on vascular K+ currents. *Br. J. Pharmacol.* **155**, 62–72
47. Jabeen, Q., Bashir, S., Lyoussi, B., and Gilani, A. H. (2009) Coriander fruit exhibits gut modulatory, blood pressure lowering and diuretic activities. *J. Ethnopharmacol.* **122**, 123–130
48. Lehman, A., Thouta, S., Mancini, G. M. S., Naidu, S., van Slegtenhorst, M., McWalter, K., Person, R., Mwenifumbo, J., Salvarinova, R., Guella, I., McKenzie, M. B., Datta, A., Connolly, M. B., Kalkhoran, S. M., Poburko, D., Friedman, J. M., Farrer, M. J., Demos, M., Desai, S., and Claydon, T.; CAUSES Study; EPGEN Study. (2017) Loss-of-function and gain-of-function mutations in KCNQ5 cause intellectual disability or epileptic encephalopathy. *Am. J. Hum. Genet.* **101**, 65–74
49. Rosti, G., Tassano, E., Bossi, S., Divizia, M. T., Ronchetto, P., Servetti, M., Lerone, M., Pisciotta, L., Mancardi, M. M., Veneselli, E., and Puliti, A. (2018) Intragenic duplication of KCNQ5 gene results in aberrant splicing leading to a premature termination codon in a patient with intellectual disability. *Eur. J. Med. Genet.* **18**, S1769-7212(18)30481-6
50. Lau, E., Kossidas, K., Kim, T. Y., Kunitomo, Y., Ziv, O., Song, Z., Taylor, C., Schofield, L., Yammine, J., Liu, G., Peng, X., Qu, Z., Koren, G., and Choi, B. R. (2015) Spatially discordant alternans and arrhythmias in tachypacing-induced cardiac myopathy in transgenic LQT1 rabbits: the importance of IKs and Ca2+ cycling. *PLoS One* **10**, e0122754; erratum: e0132198
51. Dhyani, N., Parveen, A., Siddiqi, A., Hussain, M. E., and Fahim, M. (2018) Cardioprotective efficacy of Coriandrum sativum (L.) seed extract in heart failure rats through modulation of endothelin receptors and antioxidant potential. [E-pub ahead of print] *J. Diet. Suppl.* 10.1080/19390211.2018.1481483
52. Walker, N. M., Flagella, M., Gawenis, L. R., Shull, G. E., and Clarke, L. L. (2002) An alternate pathway of cAMP-stimulated Cl secretion across the NKCC1-null murine duodenum. *Gastroenterology* **123**, 531–541
53. Jepps, T. A., Greenwood, I. A., Moffatt, J. D., Sanders, K. M., and Ohya, S. (2009) Molecular and functional characterization of Kv7 K+ channel in murine gastrointestinal smooth muscles. *Am. J. Physiol. Gastrointest. Liver Physiol.* **297**, G107–G115
54. Miceli, F., Soldovieri, M. V., Ambrosino, P., Barrese, V., Migliore, M., Cilio, M. R., and Taglialatela, M. (2013) Genotype-phenotype correlations in neonatal epilepsies caused by mutations in the voltage sensor of K(v)7.2 potassium channel subunits. *Proc. Natl. Acad. Sci. USA* **110**, 4386–4391
55. Amato, G., Roeloffs, R., Rigdon, G. C., Antonio, B., Mersch, T., McNaughton-Smith, G., Wickenden, A. D., Fritch, P., and Suto, M. J. (2011) N-pyridyl and pyrimidine benzamides as KCNQ2/Q3 potassium channel openers for the treatment of epilepsy. *ACS Med. Chem. Lett.* **2**, 481–484
56. Brueggemann, L. I., Haick, J. M., Cribbs, L. L., and Byron, K. L. (2014) Differential activation of vascular smooth muscle Kv7.4, Kv7.5, and Kv7.4/7.5 channels by ML213 and ICA-069673. *Mol. Pharmacol.* **86**, 330–341
57. Wickenden, A. D., Krajewski, J. L., London, B., Wagoner, P. K., Wilson, W. A., Clark, S., Roeloffs, R., McNaughton-Smith, G., and Rigdon, G. C. (2008) N-(6-chloro-pyridin-3-yl)-3,4-difluoro-benzamide (ICA-27243): a novel, selective KCNQ2/Q3 potassium channel activator. *Mol. Pharmacol.* **73**, 977–986
58. Kubo, I., Fujita, K., Kubo, A., Nihei, K., and Ogura, T. (2004) Antibacterial activity of coriander volatile compounds against Salmonella choleraesuis. *J. Agric. Food Chem.* **52**, 3329–3332
59. Zviely, M. (2009) Molecule of the month: trans-2-dodecenal. *Perfum. Flavor.* **34**, 26–28

Received for publication February 18, 2019.
Accepted for publication June 25, 2019.